Table I. *Patients' characteristics.*

	Docetaxel + carboplatin c (%) (n=60)	Paclitaxel + arboplatin (%) (n=30)
Age (median) (years)	67.5	65.5
Male/female	43/13 (78/22)	22/8 (73/27)
Body weight loss>5% Yes /no	11/49 (18/82)	5/25 (17/83)
Performance status 0/1	19/41 (32/68)	7/23 (23/77)
Histology Sq/Ad/La/Other	13/36/2/9 (22/60/3/15)	10/17/0/3 (33/57/0/10)
Stage IIIB/IV	24/36 (40/60)	10/20 (33/67)
Naïve/relapsed	53/7 (88/12)	26/4 (87/13)
LDH Normal/abnormally high	44/16 (73/27)	21/9 (70/30)
Prior radiotherapy	3 (5)	3 (10)

Sq: Squamous cell carcinoma, Ad: adenocarcinoma, La: large cell carcinoma, LDH: lactate dehydrogenase.

Table II. *Overall response and survival data.*

Regimen	Docetaxel + carboplatin	Paclitaxel + carboplatin
Number of patients	60	30
Response rate (95%CI)	23% (13-36%)	33% (17-53%)
Median PFS (95% CI), months	4.8 (3.9-7.2)	5.1 (4.4-6.4)
PFS rate (90% CI)*	42% (31-52)	40% (25-54)
HR (95% CI)	0.86 (0.55-1.36)	Referent
Median OS (95% CI), months	17.6 (10.2-23.0)	15.5 (9.4-20.8)
HR (95% CI)	0.77 (0.47-1.26)	Referent
1-Year survival rate (90% CI)	60% (49-70)	60% (44-73)

MST: Median survival time, CI: confidence interval, HR: hazard ratio, PFS: progression-free survival , OS: overall survival. *At six months.

Table III. *Toxicities experienced during study period.*

Toxicity	Docetaxel+ carboplatin % (95% CI) N=60	Paclitaxel+ carboplatin % (95% CI) N=30
Grade 3 or more Neutropenia	88 (77-95)	60 (41-77)
Grade 3 or more Anemia (hemoglobin)	12 (5-23)	7 (1-22)
Grade 3 or more Thrombocytopenia	0	3 (0-17)
Grade 3 or more Frbrile neutropenia	17 (8-29)	13 (4-31)
Grade 2 or more Nausea	28 (18-41)	17 (6-35)
Grade 2 or more Vomiting	12 (5-23)	10 (2-27)
Grade 2 or more Sensory neuropathy	3 (0-12)	37 (20-56)
Grade 2 or more Myalgia	0	13 (4-31)
Grade 2 or more Arthralgia	2 (0-9)	20 (8-39)
Possible TRD (ARDS)	1	0

CI: Confidence interval, TRD: treatment-related death, ARDS: acute respiratory distress syndrome.

or time to progression was 4.8, 5.8, and 4.5 months, and the MST was 13.3, 14.1, and 12.3 months, respectively. These results are similar to those of the present trial, obtaining a PFS of 5.1 months and an MST of 15.6 months, and suggest that Japanese patients have a good response to taxane-based chemotherapy. C1236T polymorphism in the ATP-binding cassette sub-family B member-1 (*ABCB1*) gene is significantly related to docetaxel clearance (18). Gandara *et al.* reported ethnic differences in the metabolism of taxanes between American and Japanese patients with lung cancer in a common-arm analysis of PCarbo, performed jointly in the United States and Japan (19).

Differences in the allelic distribution of genes involved in paclitaxel disposition or DNA repair [cytochrome *P450* 3A4 (CYP3A4)*1B and excision repair cross-complementation group 2 (*ERCC2*) K751Q] were observed between Japanese and American patients. Resulting metabolic differences in taxane metabolism may consequently contribute to better outcomes in Asian patients with lung cancer who receive taxanes.

In our study the dose of docetaxel was 60 mg/m^2 and that of carboplatin was AUC 6 mg/ml min. This dose of docetaxel is generally used in Japan to treat NSCLC. When combined with cisplatin, the dose of docetaxel used in Japan may be slightly lower the one that used in other countries (6). However, the results of Japanese studies in terms of PFS or overall survival are not inferior to those of studies performed in other countries, where docetaxel is usually given at a dose of 75 mg/m^2 (7). On the other hand, most Japanese studies have used cisplatin at a dose of 80 mg/m^2, which is slightly higher than that used in other countries (75 mg/m^2). The modest differences in the doses of chemotherapeutic agents may not have had a major influence on PFS or overall survival. Brunetto *et al.* reported that the dose intensity of platinum-doublet regimens including cisplatin or carboplatin with either vinorelbine or gemcitabine did not have an impact on survival or time-to-progression in patients with NSCLC (20).

A phase III study comparing DCarbo with PCarbo as first-line chemotherapy was performed in 1,077 patients with ovarian cancer (21). Docetaxel (75 mg/m^2) or paclitaxel (175 mg/m2) with carboplatin to (AUC 5 mg/ml min) was administered every three weeks for six cycles.

The study also concluded that DCarbo is similar to PCarbo in terms of PFS and response, but recommended that longer follow-up is required before making a definitive statement on survival. DCarbo was considered an alternative first-line regimen for chemotherapy in patients with ovarian cancer. As for toxicity, DCarbo was associated with

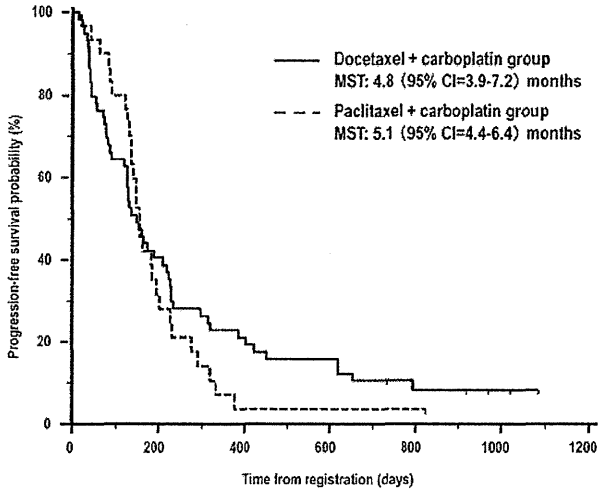

Figure 2. *Progression-free survival. MST: Median survival time, CI: confidence interval.*

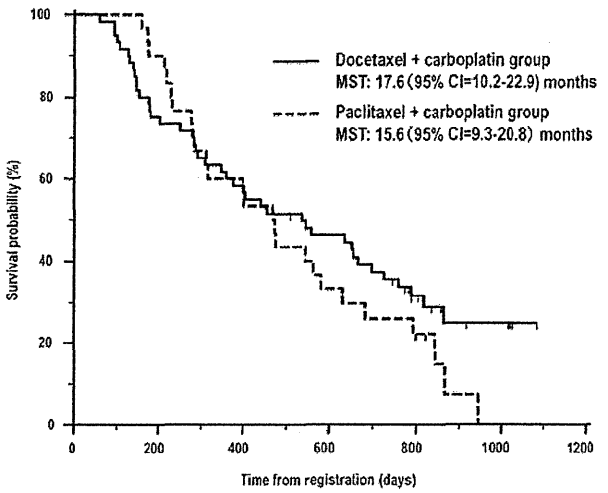

Figure 3. *Overall survival. MST: Median survival time, CI: confidence interval.*

substantially less overall and grade 2 or more neurotoxicity than PCarbo. On the other hand, DCarbo led to a higher incidence of grade 3 or 4 neutropenia than did PCarbo. Similar trends were noted in our study: DCarbo had a lower incidence of grade 2 or more sensory neuropathy (3% *vs.* 37%), but a higher incidence of grade 3 or more neutropenia (87% *vs.* 60%) as compared with PCarbo. Although myelosuppression was also frequently associated with DCarbo in our study, this adverse effect was not dose-limiting.

Recently, the survival of patients with NSCLC has improved, in part because of improved treatments or perhaps because of selection bias. The longer the survival, the more problematic is chronic toxicity such as neurotoxicity. Such toxicity negatively affects the quality of life of patients with NSCLC. This is especially true for those tested with PCarbo regimens (22). Even if the dose of paclitaxel is reduced from 225 mg/m^2 to 200 mg/m^2, the problem of neurotoxicity persists. DCarbo would, thus, be the preferred regimen to avoid severe neurotoxicity.

The treatment-related death in the DCarbo group in our study was reviewed by a safety committee. ARDS occurred as late as two months after the end of the patient's fifth, final cycle of treatment. The relation of death to chemotherapy with DCarbo was considered not definite, but possible.

Our study had several important limitations. We studied only Japanese patients, and it remains unclear whether our results can be extrapolated to other ethnic groups. Our study group comprised of patients with all histological types of NSCLC, and information on mutations in the *EGFR* gene was not obtained. In addition, the doses of docetaxel and carboplatin differed from those used in Western studies of patients with NSCLC.

Conclusion

Docetaxel plus carboplatin is considered an alternative first-line chemotherapeutic regimen for patients with newly-diagnosed advanced NSCLC, at least in Asia. In the future, this regimen might be combined with other treatments, such as molecular targeted therapy.

Conflicts of Interest

None.

Acknowledgements

We are indebted to the late Kiyoyuki Furuse, MD, who contributed to the data management of this study.

References

1 Siegel R, Naishadham D and Jemal A: Cancer statistics, 2013. CA Cancer J Clin *63*: 11-30, 2013.

2 Mitsudomi T, Morita S, Yatabe Y, Negoro S, Okamoto I, Tsurutani J, Seto T, Satouchi M, Tada H, Hirashima T, Asami K, Katakami N, Takada M, Yoshioka H, Shibata K, Kudoh S, Shimizu E, Saito H, Toyooka S, Nakagawa K, Fukuoka M, West Japan Oncology Group: Gefitinib *versus* cisplatin plus docetaxel in patients with non-small-cell lung cancer harbouring mutations of the epidermal growth factor receptor (WJTOG3405): An open label, randomised phase III trial. Lancet Oncol *11*: 121-128, 2010.

3 Maemondo M, Inoue A, Kobayashi K, Sugawara S, Oizumi S, Isobe H, Gemma A, Harada M, Yoshizawa H, Kinoshita I, Fujita Y, Okinaga S, Hirano H, Yoshimori K, Harada T, Ogura T, Ando M, Miyazawa H, Tanaka T, Saijo Y, Hagiwara K, Morita S, Nukiwa T, North-East Japan Study Group: Gefitinib or chemotherapy for non-small-cell lung cancer with mutated *EGFR*. N Engl J Med *362*: 2380-2388, 2010.

4 Buettner R, Wolf J and Thomas RK: Lessons learned from lung cancer genomics: The emerging concept of individualized diagnostics and treatment. J Clin Oncol *31*: 1858-1865, 2013.

5 Kwak EL, Bang YJ, Camidge DR, Shaw AT, Solomon B, Maki RG, Ou SH, Dezube BJ, Janne PA, Costa DB, Varella-Garcia M, Kim WH, Lynch TJ, Fidias P, Stubbs H, Engelman JA, Sequist LV, Tan W, Gandhi L, Mino-Kenudson M, Wei GC, Shreeve SM, Ratain MJ, Settleman J, Christensen JG, Haber DA, Wilner K, Salgia R, Shapiro GI, Clark JW and Iafrate AJ: Anaplastic lymphoma kinase inhibition in non-small cell lung cancer. N Engl J Med *363*: 1693-1703, 2010.

6 Kubota K, Watanabe K, Kunitoh H, Noda K, Ichinose Y, Katakami N, Sugiura T, Kawahara M, Yokoyama A, Yokota S, Yoneda S, Matsui K, Kudo S, Shibuya M, Isobe T, Segawa Y, Nishiwaki Y, Ohashi Y and Niitani H: Phase III randomized trial of docetaxel plus cisplatin *versus* vindesine plus cisplatin in patients with stage IV non-small cell lung cancer: the Japanese Taxotere Lung Cancer Study Group. J Clin Oncol *22*: 254-261, 2004.

7 Fossella F, Pereira JR, von Pawel J, Pluzanska A, Gorbounova V, Kaukel E, Mattson KV, Ramlau R, Szczesna A, Fidias P, Millward M and Belani CP: Randomized, multinational, phase III study of docetaxel plus platinum combinations *versus* vinorelbine plus cisplatin for advanced non-small-cell lung cancer: The TAX 326 study group. J Clin Oncol *21*: 3016-3024, 2003.

8 Millward MJ, Boyer MJ, Lehnert M, Clarke S, Rischin D, Goh BC, Wong J, McNeil E and Bishop JF: Docetaxel and carboplatin is an active regimen in advanced non-small cell lung cancer: A phase II study in Caucasian and Asian patients. Ann Oncol *14*: 449-454, 2003.

9 Kasahara K, Kimura H, Shibata K, Araya T, Sone T, Oribe Y, Furusho S, Kita T, Shirasaki H, Yoshimi Y, Ueda A, Tachibana H, Shintani H, Mizuguchi M, Nishi K, Fujimura M and Nakao S: A phase II study of combination chemotherapy with docetaxel and carboplatin for patients with advanced or metastatic non-small cell lung cancer. Anticancer Res *26*: 3723-3728, 2006.

10 Kataoka K, Suzuki R, Taniguchi H, Noda Y, Shindoh J, Matsumoto S, Watanabe Y, Honda K, Suzuki K, Baba K, Imaizumi K, Kume H, Hasegawa Y and Takagi K: Phase I/II trial of docetaxel and carboplatin as a first-line therapy in patients with stage IV non-small cell lung cancer. Lung *184*: 133-139, 2006.

11 Cockcroft DW and Gault MH: Prediction of creatinine clearance from serum creatinine. Nephron *16*: 31-41, 1976.

12 Pocock SJ and Simon R: Sequential Treatment Assignment with Balancing for Prognostic Factors in the Controlled Clinical Trial. Biometrics *31*: 103-115, 1975.

13 Therasse P, Arbuck SG, Eisenhauer EA, Wanders J, Kaplan RS, Rubinstein L, Verweij J, Van Glabbeke M, van Oosterom AT, Christian MC and Gwyther SG: New guidelines to evaluate the response to treatment in solid tumors. European Organization for Research and Treatment of Cancer, National Cancer Institute of the United States, National Cancer Institute of Canada. J Natl Cancer Inst *92*: 205-216, 2000.

14 NCI-CTC v2.0, 1999: http://ctep.cancer.gov/

15 Okamoto I, Yoshioka H, Morita S, Ando M, Takeda K, Seto T, Yamamoto N, Saka H, Asami K, Hirashima T, Kudoh S, Satouchi M, Ikeda N, Iwamoto Y, Sawa T, Miyazaki M, Tamura K, Kurata T, Fukuoka M and Nakagawa K: Phase III trial comparing oral S-1 plus carboplatin with paclitaxel plus carboplatin in chemotherapy-naive patients with advanced non-small cell lung cancer: Results of a West Japan Oncology Group study. J Clin Oncol *28*: 5240-5246, 2010.

16 Kubota K, Kawahara M, Ogawara M, Nishiwaki Y, Komuta K, Minato K, Fujita Y, Teramukai S, Fukushima M and Furuse K: Vinorelbine plus gemcitabine followed by docetaxel *versus* carboplatin plus paclitaxel in patients with advanced non-small cell lung cancer: A randomised, open-label, phase III study. Lancet Oncol *9*: 1135-1142, 2008.

17 Ohe Y, Ohashi Y, Kubota K, Tamura T, Nakagawa K, Negoro S, Nishiwaki Y, Saijo N, Ariyoshi Y and Fukuoka M: Randomized phase III study of cisplatin plus irinotecan *versus* carboplatin plus paclitaxel, cisplatin plus gemcitabine, and cisplatin plus vinorelbine for advanced non-small cell lung cancer: Four-Arm Cooperative Study in Japan. Ann Oncol *18*: 317-323, 2007.

18 Bosch TM, Huitema AD, Doodeman VD, Jansen R, Witteveen E, Smit WM, Jansen RL, van Herpen CM, Soesan M, Beijnen JH and Schellens JH: Pharmacogenetic screening of CYP3A and ABCB1 in relation to population pharmacokinetics of docetaxel. Clin Cancer Res *12*: 5786-5793, 2006.

19 Gandara DR, Kawaguchi T, Crowley J, Moon J, Furuse K, Kawahara M, Teramukai S, Ohe Y, Kubota K, Williamson SK, Gautschi O, Lenz HJ, McLeod HL, Lara PN Jr., Coltman CA, Jr., Fukuoka M, Saijo N, Fukushima M and Mack PC: Japanese-US common-arm analysis of paclitaxel plus carboplatin in advanced non-small cell lung cancer: A model for assessing population-related pharmacogenomics. J Clin Oncol *27*: 3540-3546, 2009.

20 Brunetto AT, Carden CP, Myerson J, Faria AL, Ashley S, Popat S and O'Brien ME: Modest reductions in dose intensity and drug-induced neutropenia have no major impact on survival of patients with non-small cell lung cancer treated with platinum-doublet chemotherapy. J Thorac Oncol *5*: 1397-1403, 2010.

21 Vasey PA: Role of docetaxel in the treatment of newly diagnosed advanced ovarian cancer. J Clin Oncol *21*: 136s-144s, 2003.

22 Rigas JR: Taxane-platinum combinations in advanced non-small cell lung cancer: A review. Oncologist *9(Suppl 2)*: 16-23m, 2004.

Received July 18, 2013
Revised September 13, 2013
Accepted September 16, 2013

Cellular Physiology and Biochemistry

Cell Physiol Biochem 2013;31:905-913
DOI: 10.1159/000350108
Published online: June 17, 2013
Accepted: May 21, 2013

Karger Open access

1421-9778/13/0316-0905$38.00/0

Original Paper

Crosstalk between PI3 Kinase/PDK1/Akt/Rac1 and Ras/Raf/MEK/ERK Pathways Downstream PDGF Receptor

Emma Tabe Eko Niba[a,e] Hisao Nagaya[b,e] Takeshi Kanno[a] Ayako Tsuchiya[a] Akinobu Gotoh[b] Chiharu Tabata[c] Kohzo Kuribayashi[d] Takashi Nakano[c] Tomoyuki Nishizaki[a]

[a]Division of Bioinformation, Department of Physiology, Hyogo College of Medicine, Nishinomiya; [b]Laboratory of Cell and Gene Therapy, Institute for Advanced Medical Sciences, Hyogo College of Medicine, Nishinomiya; [c]Department of Thoracic Oncology, Hyogo College of Medicine, Nishinomiya; [d]Department of Respiratory Internal Medicine, Murakami Memorial Hospital, Asahi University School of Dentistry, Gifu; [e]E.T.E. Niba and H. Nagaya contributed equally to this work

Key Words
PDGF-ββ receptor • Akt • Rac1 • ERK • Crosstalk

Abstract
Background/Aims: Our earlier studies suggested crosstalk between IRS/PI3 kinase/PDK1/Akt/Rac1/ROCK and (Shc2/Grb2/SOS)/Ras/Raf/MEK/ERK pathways downstream PDGF-ββ receptor responsible for chemotaxis and proliferation of malignant mesothelioma cells. The present study was conducted to obtain evidence for this. ***Methods:*** To assess activation of Akt, MEK, and ERK, Western blotting was carried out on MSTO-211H malignant mesothelioma cells using antibodies against phospho-Thr308-Akt, phopho-Ser473-Akt, Akt, phospho-MEK, MEK, phopho-ERK1/2, and ERK1/2. To knock-down Akt, PI3 kinase, PDK1, and Rac1, siRNAs silencing each-targeted gene were constructed and transfected into cells. To monitor Rac1 activity, FRET monitoring was carried out on living and fixed cells. ***Results:*** ERK was activated under the basal conditions in MSTO-211H cells, and the activation was prevented by inhibitors for PI3 kinase, PDK1, Akt, and Rac1 or by knocking-down PI3 kinase, PDK1, Akt, and Rac1. Akt was also activated under the basal conditions, and the activation was suppressed by a MEK inhibitor and an ERK1/2 inhibitor. In the FRET analysis, Rac1 was activated under the basal conditions, and the activation was inhibited by a MEK inhibitor and an ERK1/2 inhibitor. ***Conclusion:*** The results of the present study show that ERK could be activated by PI3 kinase, PDK1, Akt, and Rac1 and that alternatively, Akt and Rac1 could be activated by MEK and ERK in MSTO-211H cells.

Prof. Tomoyuki Nishizaki

Division of Bioinformation, Department of Physiology, Hyogo College of Medicine
1-1 Mukogawa-cho, Nishinomiya 663-8501 (Japan)
Tel. +81-798-45-6397, Fax +81-798-45-6649, E-Mail tomoyuki@hyo-med.ac.jp

Introduction

Platelet-derived growth factor (PDGF) promotes proliferation of malignant mesothelioma cells as well as other cancer types of cells [1-6]. The PDGF family includes PDGF-A, -B, -C and -D. PDGF-A and -B are secreted as active dimers composed of single-domain protein chains (PDGF-AA and -BB), but otherwise PDGF-C and -D, which contain an N-terminal CUB and a conserved C-terminal growth factor domain, are secreted as a latent dimeric factor and undergo proteolytic processing at the hinge region between the CUB domain and the growth factor domain to produce the active form of PDGF-CC and -DD through tissue plasminogen activator (tPA) and urokinase-type plasminogen activator (uPA), respectively [7-9]. PDGF receptors consist of the PDGF-α and/or -β subunit such as $\alpha\alpha$ homodimer, $\alpha\beta$ heterodimer, and $\beta\beta$ homodimer [7]. PDGF-$\alpha\alpha$ and -$\alpha\beta$ receptors are activated by PDGF-AA, -BB, and -CC, and PDGF-$\beta\beta$ receptor is activated by PDGF-DD [8, 9].

In our earlier studies, PDGF-D, endogenously secreted, facilitated chemotaxis and promoted proliferation of malignant mesothelioma cells through PDGF-$\beta\beta$ receptor [10, 11]. PDGF-$\beta\beta$ receptor is a receptor tyrosine kinase, which phosphorylates the receptor by itself and insulin receptor substrate protein (IRS). IRS, in turn, recruits and activates phosphoinositide 3-kinase (PI3 kinase), to produce phosphatidylinositol (3,4,5)-trisphosphate [PI (3,4,5) P_3] from phosphatidylinositol (4,5)-biphosphate [PI (4,5) P_2]. PI (3,4,5) P_3 binds to and activates phosphoinositide-dependent kinase-1 (PDK1), which phosphorylates and activates Akt. Akt activates the Rho family Rac1/Cdc42, followed by activation of the effector Rho-associated coiled-coil forming protein kinase (ROCK). PDGF-$\beta\beta$ receptor, alternatively, phosphorylates Shc2, which forms a complex of Shc2/Grb2/SOS to activate Ras. Ras subsequently activates Raf followed by the sequent phosphorylation and activation of mitogen-activated protein (MAP) kinase cascades such as MAP kinase kinase (MEK) and extracellular signal-regulated kinase (ERK). Spontaneous proliferation of malignant mesothelioma cells was clearly suppressed by knocking-down PDGF-D and PDGF-$\beta\beta$ receptor [11]. The proliferation was significantly inhibited by the Akt inhibitor MK2206, and the ROCK inhibitor Y27632, but amazingly the PI3 kinase inhibitor wortmannin, the PDK1 inhibitor BX912, or the Rac1 inhibitor NSC23766 had no effect [11]. This suggests that Akt or ROCK is not activated along a PDGF-$\beta\beta$ receptor/PI3 kinase/PDK1/Akt/Rac1/ROCK axis. Moreover, proliferation of MSTO-211H cells was still inhibited by the MEK inhibitor PD98059 and the ERK1/2 inhibitor FR180204. Then, we hypothesized that crosstalk between IRS/PI3 kinase/PDK1/Akt/Rac1/ROCK and (Shc2/Grb2/SOS)/Ras/Raf/MEK/ERK pathways underlies downstream PDGF-$\beta\beta$ receptor in MSTO-211H cells.

To prove this hypothesis, the present study monitored activities of Akt and MEK/ERK by Western blotting and Rac1 using a plasmid encoded föerster resonance energy transfer (FRET) probe in MSTO-211H cells, a biphasic human malignant mesothelioma cell line. We show here that PI3 kinase, PDK1, Akt, and Rac1 could activate ERK in MSTO-211H cells and that MEK and ERK could otherwise activate Akt and Rac1.

Materials and Methods

Cell culture

MSTO-211H cell line was purchased from American Type Culture Collection (Manassas, VA, USA). Cells were grown in RPMI-1640 medium supplemented with 10% (v/v) heat-inactivated FBS, 0.003% (w/v) L-glutamine, penicillin (final concentration, 100 U/ml), and streptomycin (final concentration, 0.1 mg/ml), in a humidified atmosphere of 5% CO_2 and 95% air at 37 °C.

Western blotting

MSTO-211H cells were untreated and treated with a variety of inhibitors or transfected with small interfering RNAs (siRNAs), and then lysed in a lysate solution [150 mM NaCl, 20 mM Tris, 0.1% (v/v) Tween-20 and 0.1% (w/v) sodium dodecyl sulfate (SDS), pH 7.5] containing 1% (v/v) protease inhibitor

cocktail and 1% (v/v) phosphatase inhibitor cocktail. The lysates were centrifuged at 3,000 rpm for 5 min at 4 °C. Proteins were separated by SDS–polyacrylamide gel electrophoresis (SDS–PAGE) using a TGX gel (BioRad; Hercules, CA, USA) and then transferred to polyvinylidene difluoride (PVDF) membranes. Blotting membranes were blocked with TBS-T [150 mM NaCl, 0.1% (v/v) Tween-20 and 20 mM Tris, pH 7.5] containing 5% (w/v) bovine serum albumin and subsequently reacted with antibodies against phospho-Thr308-Akt (pT308)(Cell Signaling Technology, Inc.; Danvers, MA, USA), phospho-Ser473-Akt (pS473)(Cell Signaling Technology), Akt (Cell Signaling Technology), phospho-MEK (pMEK)(Cell Signaling Technology), MEK (Cell Signaling Technology), phospho-ERK (pERK)(Santa Cruz Biotechnology; Santa Cruz, CA, USA), ERK (Santa Cruz Biotechnology), PI3 kinase (Sigma-Aldrich; St. Louis, MO, USA), PDK1 (Sigma-Aldrich), Rac1 (Sigma-Aldrich), and β-actin (Sigma-Aldrich). After washing, membranes were reacted with a horseradish peroxidase-conjugated goat anti-mouse IgG or goat anti-rabbit IgG antibody. Immunoreactivity was detected with an ECL kit (GE healthcare; Piscataway, NJ, USA) and visualized using a chemiluminescence LAS-4000mini detection system (GE healthcare). Protein concentrations for each sample were determined with a BCA protein assay kit (Thermo Fisher Scientific; Waltham, MA, USA).

Construction and transfection of siRNA

The siRNA to silence the Akt1/2-targeted gene (Akt siRNA) was purchased from Santa Cruz Biotechnology. The siRNAs to silence the PI3 kinase p110δ-targeted gene (PI3K KD), the PDK1-targeted gene (PDK1 KD), the Rac1-targeted gene (Rac1 KD) were obtained from Ambion (Carlsbad, CA, USA). The sequences of siRNAs used were 5'-GUGAGAAAUUUGAACGGUUtt -3' and 5'-AACCGUUCAAAUUUCUCACta-3' for PI3 kinase p110δ; 5'-GGACACCAUCCGUUCAAUUtt-3' and 5'-AAUUGAACGGAUGGUGUCCtg-3' for PDK1; and 5'-CUACUGUCUUUGACAAUUAtt-3' and 5'-UAAUUGUCAAAGACAGUAGgg-3' for Rac1. Each negative control siRNA (NC siRNA)(Ambion) had the scrambled sequence, the same GC content, and nucleic acid composition. siRNAs were transfected into cells using a Lipofectamine reagent (Invitrogen; Carlsbad, CA, USA). Cells were used for experiments 48 h after transfection.

Monitoring of Rac1 activity

FRET probe containing Raichu-Rac1 with EV linker was kindly gifted from Dr. Matsuda (Kyoto university)[12, 13]. MSTO-211H cells were transfected with the FRET probe using an X-tremeGENE HP DNA transfection reagent (Roche, Mannheim, Germany). Twenty-four h after transfection fluorescent signals in living cells were monitored at 485-nm argon laser for cyan fluorescent protein (CFP) and 517-nm argon laser for yellow fluorescent protein (YFP) in the presence and absence of inhibitors with a Zeiss LSM510 META inverted microscope (Oberkochen, Germany). In a different set of experiments, cells were untreated and treated with inhibitors for periods of time, and then fixed with formaldehyde [final conc. 3.7 (v/v) %] for 30 min. Then, CFP and YFP signals were monitored. The background was subtracted and the FRET ratio (YFP signal intensity/CFP signal intensity) was calculated using an ImageJ software (National Institutes of Health, USA).

Statistical analysis

Statistical analysis was carried out using unpaired *t*-test and Dunnett's test.

Results

PI3 kinase, PDK1, Akt, and Rac1 activates ERK

ERK was phosphorylated in the absence of inhibitors in MSTO-211H cells (Fig. 1A-E), indicating that ERK is spontaneously activated under the basal conditions. The PI3 kinase inhibitor wortmannin (10 μM) [14] reduced ERK phosphorylation (Fig. 1A). Expression of PI3 kinase was suppressed in MSTO-211H cells transfected with the PI3 kinase siRNA (Fig. 4A), confirming knocking-down PI3 kinase. ERK phosphorylation was significantly prevented by knocking-down PI3 kinase (Fig. 4C). It is indicated from these results that PI3 kinase has the potential to activate ERK.

The PDK1 inhibitor BX912 (100 nM) [15] significantly reduced ERK phosphorylation (Fig. 1B). Expression of PDK1 was suppressed in MSTO-211H cells transfected with the PDK1

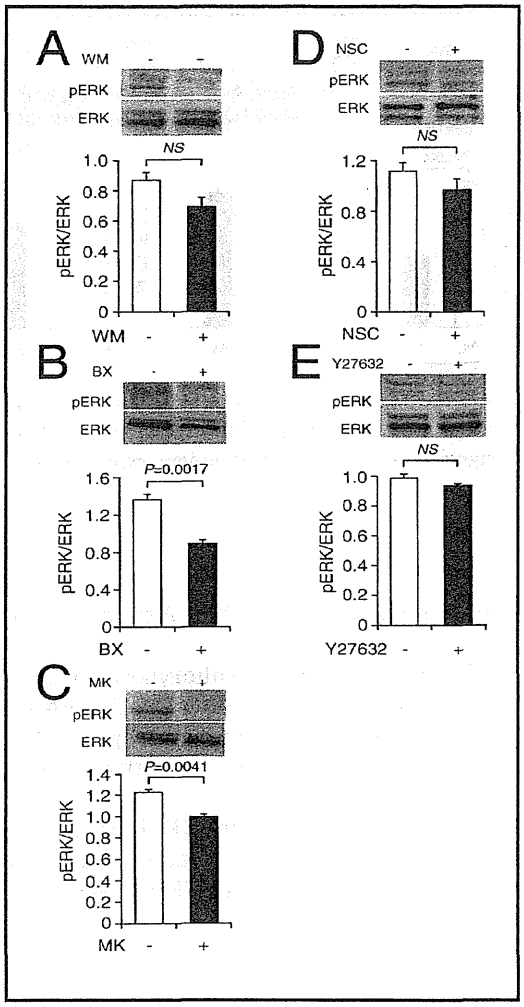

Fig. 1. ERK activation via a PI3 kinase/PDK1/Akt/Rac1 pathway. MSTO-211H cells were untreated (-) and treated (+) with wortmannin (WM)(10 μM)(A), BX912 (BX)(100 nM)(B), MK2206 (MK)(5 μM)(C), NSC23766 (NSC)(1 μM)(D), or Y27632 (10 μM)(E) for 10 min, and then, Western blotting was carried out using antibodies against pERK and ERK. In the graphs, each column represents the mean (± SEM) ratio of pERK signal intensity/ERK signal intensity (n=4 independent experiments). *P* values, Dunnett's test.

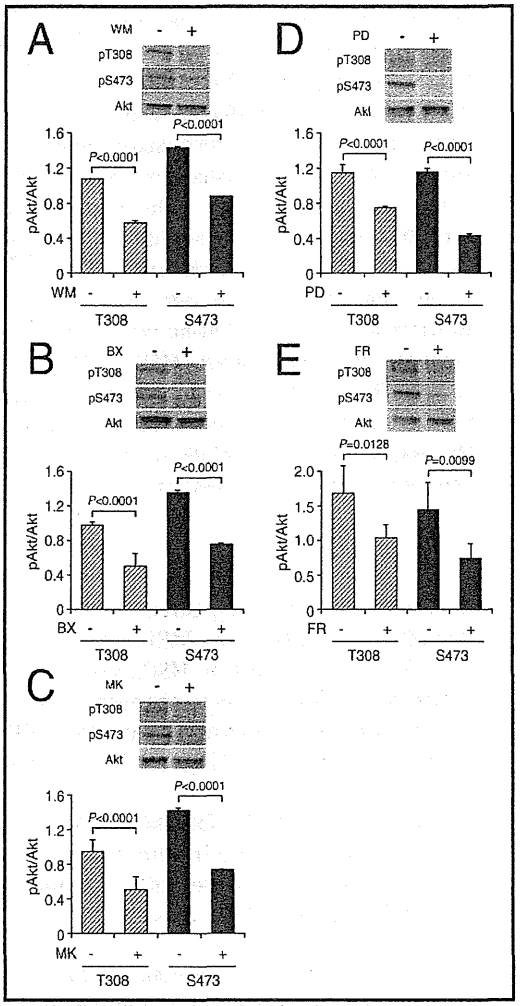

Fig. 2. Akt activation due to MEK and ERK. MSTO-211H cells were untreated (-) and treated (+) with wortmannin (WM)(10 μM)(A), BX912 (BX)(100 nM)(B), MK2206 (MK)(5 μM)(C), PD98059 (PD)(50 μM)(D), or FR180204 (FR)(10 μM)(E) for 10 min, and then, Western blotting was carried out using antibodies against pT308, pS473, and Akt. In the graphs, each column represents the mean (± SEM) ratio of pT308 signal intensity or pS473 signal intensity/Akt signal intensity (n=4 independent experiments). *P* values, Dunnett's test.

siRNA (Fig. 4D), confirming knocking-down PDK1. ERK phosphorylation was significantly prevented by knocking-down PDK1 (Fig. 4F). Collectively, these results indicate that PDK1 has the potential to activate ERK.

The Akt inhibitor MK2206 (5 μM) [16] significantly reduced ERK phosphorylation (Fig. 1C). Expression of Akt was significantly reduced in MSTO-211H cells transfected with the Akt siRNA (Fig. 3A), confirming Akt knocking-down. MEK phosphorylation was not attenuated by knocking-down Akt (Fig. 3B). Phosphorylation of ERK, on the other hand, was significantly

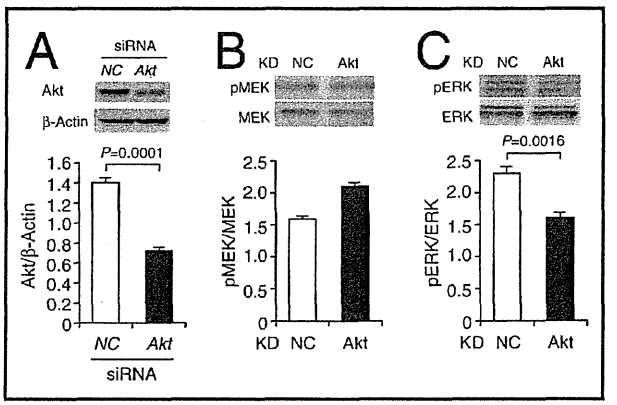

Fig. 3. Akt-mediated ERK activation. (A) Western blotting was carried out in MSTO-211H cells using antibodies against Akt and β-actin 48 h after transfection with the NC siRNA (NC) or the Akt siRNA. Signal intensities for Akt were normalized by those for β-actin. In the graph, each column represents the mean (± SEM) normalized expression of Akt (n=4 independent experiments). *P* value, unpaired *t*-test. In different sets of experiments, Western blotting was carried out using antibodies against pMEK and MEK (B) or pERK and ERK (C) 48 h after transfection with siRNAs. In the graphs, each column represents the mean (± SEM) ratio of pMEK signal intensity/MEK signal intensity or pERK signal intensity/ERK signal intensity (n=4 independent experiments). KD, knock-down. *P* value, Dunnett's test.

prevented by knocking-down Akt (Fig. 3C). These results interpret that Akt activates ERK directly, but not through MEK activation.

The Rac1 inhibitor NSC23766 (1 μM) [17] reduced ERK phosphorylation (Fig. 1D). Expression of Rac1 was suppressed in MSTO-211H cells transfected with the Rac1 siRNA (Fig. 4G), confirming knocking-down Rac1. ERK phosphorylation was significantly prevented by knocking-down Rac1 (Fig. 4I). These results indicate that Rac1 has the potential to activate ERK.

In contrast, the ROCK inhibitor Y27632 (10 μM) [18] had no effect on ERK phosphorylation (Fig. 1E), indicating no implication of ROCK in ERK activation. Taken together, these results imply that ERK could be still activated through a pathway along a PDGF-ββ receptor/PI3 kinase/PDK1/Akt/Rac1 axis.

MEK and ERK activate Akt and Rac1

Akt was phosphorylated at Thr308 and Ser473 in the absence of inhibitors in MSTO-211H cells (Fig. 2A-E), indicating that Akt is spontaneously activated under the basal conditions. Phosphorylation of Akt at Thr308 and Ser473 was inhibited by wortmannin (10 μM)(Fig. 2A) and BX912 (100 nM)(Fig. 2B). In addition, Akt phosphorylation at Thr308 and Ser473 was clearly inhibited by knocking-down PI3 kinase (Fig. 4B) and PDK1 (Fig. 4E). These results imply that Akt is activated through a pathway along a PDGF-ββ receptor/PI3 kinase/PDK1/Akt axis. Interestingly, Akt phosphorylation was also inhibited by MK2206 (5 μM)(Fig. 2C). This suggests that Akt might be activated through its autophosphorylation. Moreover, Akt phosphorylation was significantly inhibited by knocking-down Rac1 (Fig. 4H). This suggests that Rac1 is capable of activating Akt, i.e., Rac1 serves as a positive feedback activator of Akt.

Phosphorylation of Akt at Thr308 and Ser473 was also prevented by the MEK inhibitor PD98059 (50 μM) [19] (Fig. 2D) and the ERK1/2 inhibitor FR180204 (10 μM) [20, 21] (Fig. 2E). This indicates that MEK and ERK have the potential to activate Akt.

We finally monitored Rac1 activity in living and fixed MSTO-211H cells using a FRET probe. In the FRET analysis, increasing and reducing FRET ratio (YFP signal intensity/CFP signal intensity) correspond to activation and inactivation of Rac1, respectively. For living cells, the FRET ratio was apparently reduced by MK2206 (5 μM), while the ratio was not altered in the absence of inhibitors (Fig. 5A). This indicates that Rac1 is activated in an Akt-dependent manner under the basal conditions. The FRET ratio was also diminished by FR180204 (10 μM), but to a lesser extent than that for MK2206 (Fig. 5A), suggesting ERK-mediated Rac1 activation. For fixed cells, the FRET ratio was clearly inhibited by wortmannin

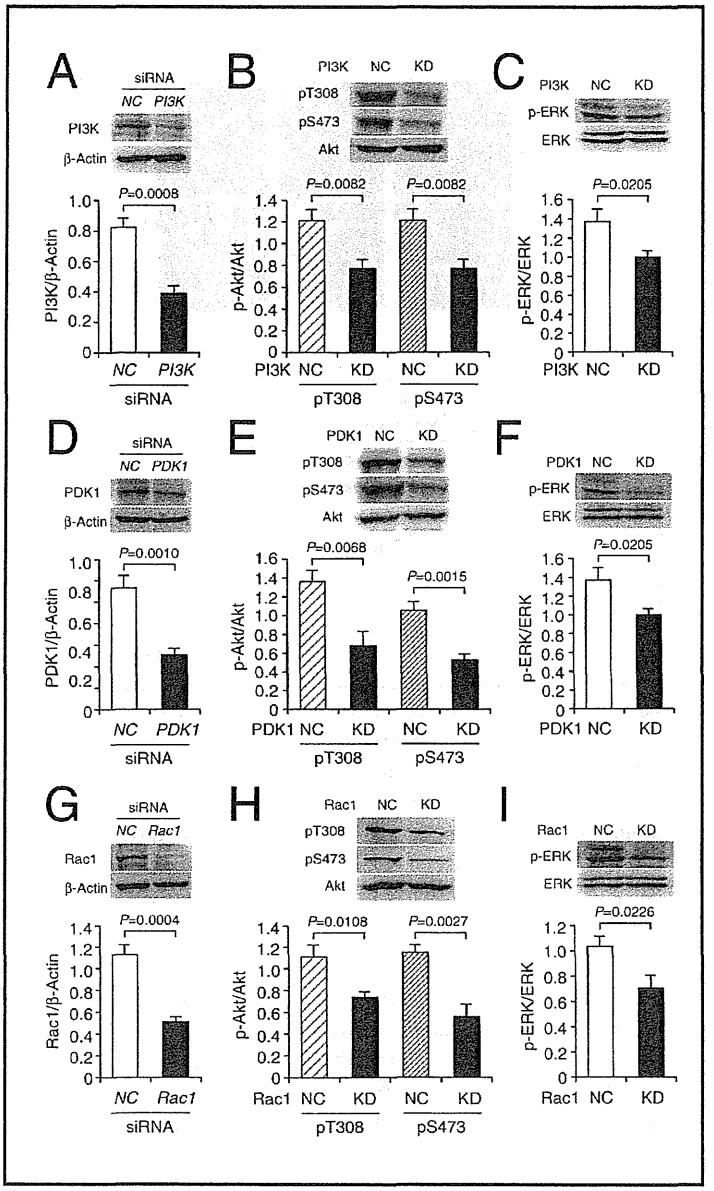

Fig. 4. ERK activation due to PI3 kinase, PDK1, and Rac1. Expression of PI3 kinase (A), PDK1 (D), and Rac1 (G) in MSTO-211H cells transfected with the NC and each siRNA. Signal intensities were normalized by those for β-actin. In the graphs, each column represents the mean (± SEM) normalized expression of PI3 kinase, PDK1, and Rac1 (n=4 independent experiments). *P* values, unpaired *t*-test. Akt activity in cells transfected with the NC siRNA, the PI3 kinase siRNA (B), the PDK1 siRNA (E), and the Rac1 siRNA (H). In the graphs, each column represents the mean (± SEM) ratio of pT308 signal intensity or pS473 signal intensity/Akt signal intensity (n=4 independent experiments). *P* values, Dunnett's test. ERK activation in cells transfected with the NC siRNA, the PI3 kinase siRNA (C), the PDK1 siRNA (F), and the Rac1 siRNA (I). In the graphs, each column represents the mean (± SEM) ratio of pERK signal intensity/ERK signal intensity (n=4 independent experiments). *P* values, Dunnett's test. PI3K, PI3 kinase; KD, knock-down.

(10 μM), BX912 (100 nM), and MK2206 (5 μM)(Fig. 5B), confirming Rac1 activation along a PI3 kinase/PDK1/Akt axis. The FRET ratio was still reduced by PD98059 (50 μM) and FR180204 (10 μM)(Fig. 5B). This indicates that Rac1 could be activated by MEK or ERK.

Discussion

PDGF-ββ receptor is implicated in two main pathways; an IRS/PI3 kinase/PDK1/Akt/Rac1/ROCK pathway and a (Shc2/Grb2/SOS)/Ras/Raf/MEK/ERK pathway (Fig. 6). In the present study, activation of Akt and ERK was found under the basal conditions in MSTO-211H biphasic human malignant mesothelioma cells. This, in the light of the fact that spontaneous proliferation of malignant mesothelioma cells was inhibited by knocking-down PDGF-D and PDGF-ββ receptor [11], indicates that Akt and ERK are activated via two main pathways linked to PDGF-ββ receptor, which is activated by PDGF-D endogenously secreted in MSTO-211H cells.

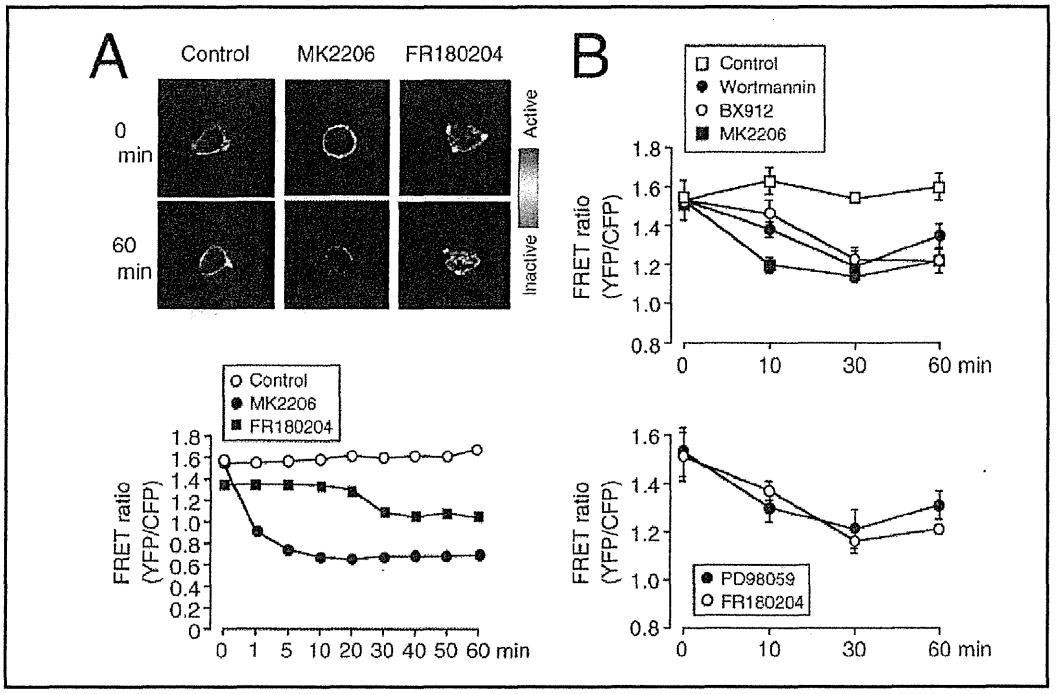

Fig. 5. Rac1 activation due to MEK and ERK. (A) FRET monitoring was carried out on living MSTO-211H cells in the absence (Control) and presence of MK2206 (5 μM) or FR180204 (10 μM), and the FRET ratio (YFP signal intensity/CFP signal intensity) was calculated. The FRET ratio images are shown in the upper panel and time-course FRET ratio profiles are shown in the graph. Note that a similar result was obtained with 6 independent experiments. (B) Cells were untreated and treated with wortmannin (10 μM), BX912 (100 nM), MK2206 (5 μM), PD98059 (50 μM), or FR180204 (10 μM) for periods of time as indicated. Subsequently, cells were fixed followed by FRET monitoring. In the graphs, each point represents the mean (± SEM) FRET ratio (n=5-10 independent experiments).

An established pathway is that ERK is activated through a pathway along a (Shc2/Grb2/SOS)/Ras/Raf/MEK/ERK axis as mediated by receptor tyrosine kinase including PDGF-ββ receptor. In the present study, ERK phosphorylation in MSTO-211H cells was prevented by inhibitors for PI3 kinase, PDK1, Akt, and Rac1 or by knocking-down PI3 kinase, PDK1, Akt, and Rac1. This indicates that ERK could be still activated through a pathway along a PDGF-ββ receptor/IRS/PI3 kinase/PDK1/Akt/Rac1 axis, regardless of a PDGF-ββ receptor/ (Shc2/Grb2/SOS)/Ras/Raf/MEK/ERK axis (Fig. 6). In other words, this shows a crosstalk activation of ERK in PDGF-ββ receptor signaling pathways (Fig. 6).

It is well-recognized that Akt is activated through a pathway along an IRS/PI3 kinase/PDK1/Akt axis as mediated by receptor tyrosine kinase including PDGF-ββ receptor. In support of this pathway,

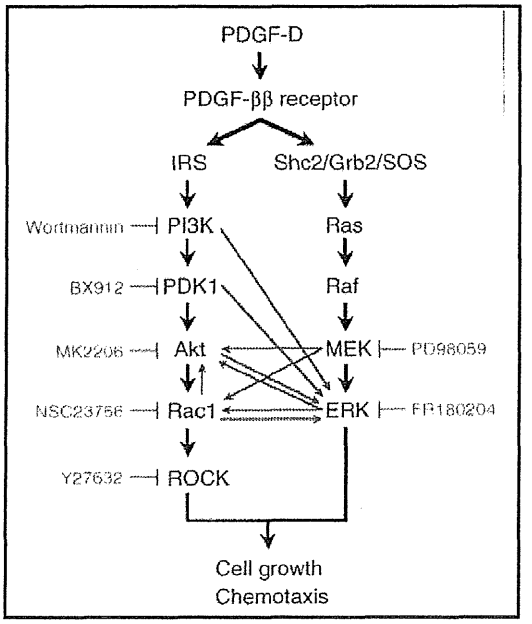

Fig. 6. A schematic diagram for crosstalk in PDGF-ββ receptor signaling pathways.

Akt phosphorylation in MSTO-211H cells was inhibited by inhibitors for PI3 kinase and PDK1 or by knocking-down PI3 kinase and PDK1. Notably, Akt phosphorylation was still inhibited by an Akt inhibitor, suggesting that Akt might be activated through its autophosphorylation. Of particular interest is the finding that Akt phosphorylation was suppressed by knocking-down Rac1. This raises the possibility that Rac1 serves as a positive feedback activator of Akt.

Akt phosphorylation was also prevented by a MEK inhibitor or an ERK inhibitor. This indicates that MEK and ERK could activate Akt via a pathway along a (Shc2/Grb2/SOS)/Ras/Raf/MEK/ERK axis as mediated by receptor tyrosine kinase including PDGF-ββ receptor (Fig. 6). In the FRET analysis, Rac1 was activated under the basal conditions in MSTO-211H cells. Expectedly, Rac1 activation was suppressed by a PI3 kinase inhibitor, a PDK1 inhibitor, and an Akt inhibitor. This provides further evidence for Rac1 activation through a pathway along a PDGF-ββ receptor/IRS/PI3 kinase/PDK1/Akt/Rac1 axis (Fig. 6). Moreover, Rac1 activation was also inhibited by a MEK inhibitor and an ERK1/2 inhibitor. This indicates that MEK and ERK could also activate Rac1 via a PDGF-ββ receptor/(Shc2/Grb2/SOS)/Ras/Raf/MEK/ERK signaling pathway (Fig. 6). Overall, these results may represent fresh insight into activation of Akt/Rac1 and ERK through crosstalk between PDGF-ββ receptor-linked two signaling pathways.

In summary, the results of the present study show that ERK could be activated through a pathway along a PDGF-ββ receptor/IRS/PI3 kinase/PDK1/Akt/Rac1 axis and that alternatively, Akt and Rac1 could be activated through a pathway along a PDGF-ββ receptor/(Shc2/Grb2/SOS)/Ras/Raf/MEK/ERK axis in MSTO-211H cells.

References

1 Garlepp MJ, Leong CC: Biological and immunological aspects of malignant mesothelioma. Eur Respir J 1995;8:643-650.
2 Upham JW, Garlepp MJ, Musk AW, Robinson BW: Malignant mesothelioma: new insights into tumour biology and immunology as a basis for new treatment approaches. Thorax 1995;50:887-893.
3 Filiberti R, Marroni P, Neri M, Ardizzoni A, Betta PG, Cafferata MA, Canessa PA, Puntoni R, Ivaldi GP, Paganuzzi M: Serum PDGF-AB in pleural mesothelioma. Tumour Biol 2005;26:221-226.
4 Versnel MA, Hagemeijer A, Bouts MJ, van der Kwast TH, Hoogsteden HC: Expression of c-sis (PDGF B-chain) and PDGF A-chain genes in ten human malignant mesothelioma cell lines derived from primary and metastatic tumors. Oncogene 1988;2:601-605.
5 Gerwin BI, Lechner JF, Reddel RR, Roberts AB, Robbins KC, Gabrielson EW, Harris CC: Comparison of production of transforming growth factor-β and platelet-derived growth factor by normal human mesothelial cells and mesothelioma cell lines. Cancer Res 1987;47:6180-6184.
6 Van der Meeren A, Seddon MB, Betsholtz CA, Lechner JF, Gerwin BI: Tumorigenic conversion of human mesothelial cells as a consequence of platelet-derived growth factor-A chain overexpression. Am J Respir Cell Mol Biol 1993;8:214-221.
7 Alvarez RH, Kantarjian HM, Cortes JE: Biology of platelet-derived growth factor and its involvement in disease. Mayo Clin Proc 2006;81:1241-1257.
8 Bergsten E, Uutela M, Li X, Pietras K, Ostman A, Heldin CH, Alitalo K, Eriksson U: PDGF-D is a specific, protease-activated ligand for the PDGF β-receptor. Nat Cell Biol 2001;3:512-516.
9 Fredriksson L, Ehnman M, Fieber C, Eriksson U: Structural requirements for activation of latent platelet-derived growth factor CC by tissue plasminogen activator. J Biol Chem 2005;280:26856-26862.
10 Okada A, Yaguchi T, Gotoh A, Nakano T, Nishizaki T: Malignant mesothelioma cell chemotaxis through a PDGF-ββ receptor signaling pathway along a PI3 kinase/PDK1/Akt/Rac1/ROCK axis. Cell Physiol Biochem 2012;29:241-250.
11 Honda M, Kanno T, Fujita Y, Gotoh A, Nakano T, Nishizaki T: Mesothelioma cell proliferation through autocrine activation of PDGF-ββ receptor. Cell Physiol Biochem 2012;29:667-674.

12 Niwa H, Yamamura K, Miyazaki J: Efficient selection for high-expression transfectants with a novel eukaryotic vector. Gene 1991;108:193-199.
13 Komatsu N, Aoki K, Yamada M, Yukinaga H, Fujita Y, Kamioka Y, Matsuda M: Development of an optimized backbone of FRET biosensors for kinases and GTPases. Mol Biol Cell 2011;22:4647-4656.
14 Rexhepaj R, Rotte A, Pasham V, Gu S, Kempe DS, Lang F: PI3 kinase and PDK1 in the regulation of the electrogenic intestinal dipeptide transport. Cell Physiol Biochem 2010;25:715-722.
15 Kloo B, Nagel D, Pfeifer M, Grau M, Düwel M, Vincendeau M, Dörken B, Lenz P, Lenz G, Krappmann D: Critical role of PI3K signaling for NF-kappaB-dependent survival in a subset of activated B-cell-like diffuse large B-cell lymphoma cells. Proc Natl Acad Sci USA 2011;108:272-277.
16 Guo JP, Coppola D, Cheng JQ: IKBKE protein activates Akt independent of phosphatidylinositol 3-kinase/PDK1/mTORC2 and the pleckstrin homology domain to sustain malignant transformation. J Biol Chem 2011;286:37389-37398.
17 Blakely BD, Bye CR, Fernando CV, Horne MK, Macheda ML, Stacker SA, Arenas E, Parish CL: Wnt5a regulates midbrain dopaminergic axon growth and guidance. PLoS One 2011;6:e18373.
18 Bianchi R, Kastrisianaki E, Giambanco I, Donato R: S100B protein stimulates microglia migration via RAGE-dependent up-regulation of chemokine expression and release. J Biol Chem 2011;286:7214-7226.
19 Filice E, Angelone T, De Francesco EM, Pellegrino D, Maggiolini M, Cerra MC: Crucial role of phospholamban phosphorylation and S-nitrosylation in the negative lusitropism induced by 17β-estradiol in the male rat heart. Cell Physiol Biochem 2011;28:41-52.
20 Jayaraman T, Tejero J, Chen BB, Blood AB, Frizzell S, Shapiro C, Tiso M, Hood BL, Wang X, Zhao X, Conrads TP, Mallampalli RK, Gladwin MT: 14-3-3 binding and phosphorylation of neuroglobin during hypoxia modulate six-to-five heme pocket coordination and rate of nitrite reduction to nitric oxide. J Biol Chem 2011;286:42679-42689.
21 Ohori M, Kinoshita T, Okubo M, Sato K, Yamazaki A, Arakawa H, Nishimura S, Inamura N, Nakajima H, Neya M, Miyake H, Fujii T: Identification of a selective ERK inhibitor and structural determination of the inhibitor-ERK2 complex. Biochem Biophys Res Commun 2005;336:357-363.

ANTICANCER RESEARCH *34*: 1759-1764 (2014)

Dipalmitoleoyl-phosphatidylethanolamine Induces Apoptosis of NCI-H28 Malignant Mesothelioma Cells

YOSHIKO KAKU[1], AYAKO TSUCHIYA[1], TAKESHI KANNO[1], TAKASHI NAKANO[2] and TOMOYUKI NISHIZAKI[1]

[1]*Division of Bioinformation, Department of Physiology, and* [2]*Division of Pulmonary Medicine, Department of Internal Medicine, Hyogo College of Medicine, Nishinomiya, Japan*

Abstract. *Background/Aim: The phospholipid phosphatidylethanolamine regulates a wide range of cellular processes. The present study investigated the antitumor effect of 1,2-dipalmitoleoyl-sn-glycero-3-phosphoethanolamine (DPPE) on malignant pleural mesothelioma cells. Materials and Methods: Activities of protein phosphatases (PPs) such as PP1, PP2A, and protein tyrosine phosphatase 1B (PTP1B) were assayed under cell-free conditions. 3-(4,5-Dimethyl-2-thiazolyl)-2,5-diphenyl-2H-tetrazolium bromide (MTT) assay, terminal deoxynucleotidyl transferase-mediated dUTP nick-end labeling (TUNEL) staining, and western blotting were carried out on the human Met5A non-malignant mesothelial cell line and NCI-H28 malignant mesothelioma cell line. Results: DPPE significantly enhanced PP2A and PTP1B activities. DPPE tended to attenuate activity of extracellular signal-regulated kinase-1 (ERK1)/ERK2, with the greater efficacy for NCI-H28 cells than that for Met5A cells. DPPE reduced NCI-H28 cell viability in a concentration (1-100 μM)-dependent manner, while it had no effect on Met5A cell viability. DPPE markedly increased TUNEL-positive cells in the NCI-H28 cell line, but otherwise induced few TUNEL-positive cells in the Met5A cell line. Conclusion: The results of the present study clearly demonstrate that DPPE induces apoptosis of NCI-H28 malignant pleural mesothelioma cells. DPPE-induced enhancement of PP2A and PTP1B activities might at least in part contribute to the apoptotic effect of DPPE.*

Malignant mesothelioma is an aggressive form of cancer that arises from mesothelial cells and may develop in the pleural space, pericardium, peritoneum, tunica vaginalis testis and ovarian epithelium (1). This type of cancer is often known to be resistant to chemotherapy. The median survival period of patients diagnosed with malignant mesothelioma is usually less than a year. Some factors have been associated with the development of malignant mesothelioma, which include asbestos, erionite, and simian virus 40 (SV40). Moreover, several genes are involved in the pathogenesis of this cancer: $p16^{INK4A}$, $p14^{ARF}$, and *neurofibromatosis type 2* (*NF2*). The genes *tumor protein 53* (*TP53*) and *phosphatase and tensin homolog deleted from chromosome 10* (*PTEN*) are still under investigation for their role in the development of malignant mesothelioma. In spite of extensive and intensive studies, no beneficial therapy or drug for malignant mesothelioma has been established and challenges for such development are continuing.

Receptor tyrosine kinase (RTK) is implicated in the activation of extracellular signal-regulated kinase 1/2 (ERK1/2), a mitogen-activated protein (MAP) kinase (MAPK), as one of the major signaling pathways (Figure 1). When activated, RTK phosphorylates its own receptor and Src-homology and collagen homology-2 (SHC2). Phosphorylated SHC2 recruits the adaptor protein growth factor receptor binding protein-2 (GRB2) and forms a complex with the exchanger factor son of sevenless (SOS); SHC2/GRB2/SOS, which activates the small G-protein RAS by exchanging GDP with GTP and activated RAS activates the effector RAF, a serine/threonine protein kinase. Activated RAF phosphorylates and activates MAP kinase kinase (MAPKK=MEK), which in turn, phosphorylate and activate MAPK (ERK1/2). ERK1/2 is recognized to promote cancer cell growth and protect cells from apoptosis. In this pathway, protein tyrosine phosphatase 1B (PTP1B), a tyrosine phosphatase, de-phosphorylates phosphorylated RTK and SHC2; in other words, PTP1B down-regulates RTK signaling (Figure 1). Protein phosphatase-2A (PP2A), a serine/threonine phosphatase, de-phosphorylates phosphorylation of MAPKKK, MAPKK, and ERK1/2; in other words, PP2A inhibits ERK1/2 activation (Figure 1).

In our preliminary study, we have found that phosphatidylethanolamines (PEs) such as 1,2-diarachidonoyl-*sn*-glycero-3-phosphoethanolamine (DAPE), 1,2-dilinoleoyl-*sn*-

Correspondence to: Professor Tomoyuki Nishizaki, MD, Ph.D., Division of Bioinformation, Department of Physiology, Hyogo College of Medicine, 1-1 Mukogawa-cho, Nishinomiya 663-8501, Japan. Tel: +81 798456397, Fax: +81 798456649, e-mail: tomoyuki@hyo-med.ac.jp

Key Words: Dipalmitoleoyl-*sn*-glycero-3-phosphoethanolamine, protein phosphatase, malignant pleural mesothelioma, apoptosis.

glycero-3-phosphoethanolamine (DLPE), 1,2-dioleoyl-*sn*-glycero-3-phosphoethanolamine (DOPE), and 1,2-dipalmitoleoyl-*sn*-glycero-3-phosphoethanolamine (DPPE) enhance PP2A and PTP1B activities, with the highest potential for DPPE. Then, we postulated that DPPE could exhibit an anti-tumor effect by suppressing MEK and ERK1/2 activities in association with PP2A and PTP1B activation. To address this hypothesis, the present study investigated the anti-tumor effect of DPPE on human malignant pleural mesothelioma cell lines.

Materials and Methods

Assay of protein phosphatase activities. Activities of protein phosphatases PP1, PP2A, and PTP1B under cell-free conditions were assayed as previously described (2). Human recombinant PP1 was purchased from New England BioLabs Inc. (Ipswich, MA, USA) and human recombinant PP2A from Millipore (Billerica, MA, USA). Human PTP1B was cloned into pGEX-6P-3 vector with a glutathione S-transferase (GST) tag at the NH_2 terminus, and expressed in competent *Escherichia coli* BL21 (DE3), suitable for transformation and protein expression. GST-fusion PTP1B was affinity-purified using glutathione sepharose 4B (GE Healthcare, Piscataway, NJ, USA). Activity of each phosphatase was assayed by reacting with *p*-nitrophenyl phosphate (pNPP)(Sigma-Aldrich, St. Louis, MO, USA) as a substrate. PP1 (1 U/well), PP2A (0.2 U/well), or PTP1B (1 μg/well) was pre-incubated at 30°C (for PP1) or 37°C (for PP2A and PTP1B) for 30 min in a reaction medium [50 mM HEPES, 100 mM NaCl, 2 mM dithiothreitol, 0.01% (v/v) Brij-35, 1 mM $MnCl_2$, pH 7.5 for PP1; 50 mM Tris-HCl, 0.1 mM EGTA, 0.1% (v/v) 2-mercaptoethanol, pH 7.0 for PP2A; and 50 mM HEPES, 1 mM EDTA, 50 mM NaCl, 1 mM dithiothreitol, pH 7.2 for PTP1B] in the presence and absence of phosphatase inhibitors or DPPE. pNPP at a concentration of 5 mM for PP1, 0.5 mM for PP2A, and 10 mM for PTP1B was then added to the reaction medium followed by 60-min incubation, and the reaction was terminated by adding 0.1 N of NaOH. De-phosphorylated pNPP was quantified at an absorbance of 405 nm with a SpectraMax PLUS384 (Molecular Devices, Sunnyvale, CA, USA).

Cell culture. NCI-H28 cell, a human malignant pleural mesothelioma cell line, and Met5A, a human non-malignant mesothelial cell line, were purchased from the American Type Culture Collection (Manassas, VA, USA), and cultured by the method previously described (3). Briefly, cells were grown in RPMI-1640 medium supplemented with 10% (v/v) heat-inactivated fetal bovine serum (FBS), 0.003% (w/v) L-glutamine, penicillin (final concentration, 100 U/ml), and streptomycin (final concentration, 0.1 mg/ml), in a humidified atmosphere of 5% CO_2 and 95% air at 37°C.

Cell viability assay. Cell viability was evaluated by the method using 3-(4,5-dimethyl-2-thiazolyl)-2,5-diphenyl-2*H*-tetrazolium bromide (MTT) as previously described (4).

Terminal deoxynucleotidyl transferase-mediated dUTP nick-end labeling (TUNEL) staining. TUNEL staining was performed to detect *in situ* DNA fragmentation as a marker of apoptosis using an In Situ Apoptosis Detection Kit (Takara Bio, Otsu, Japan). Briefly, fixed and permeabilized cells were reacted with terminal deoxynucleotidyl transferase and fluorescein isothiocyanate (FITC)-deoxyuridine triphosphate for 90 min at 37°C. FITC signals were visualized with a confocal scanning laser microscope (LSM 510; Carl Zeiss Co., Ltd., Oberkochen, Germany).

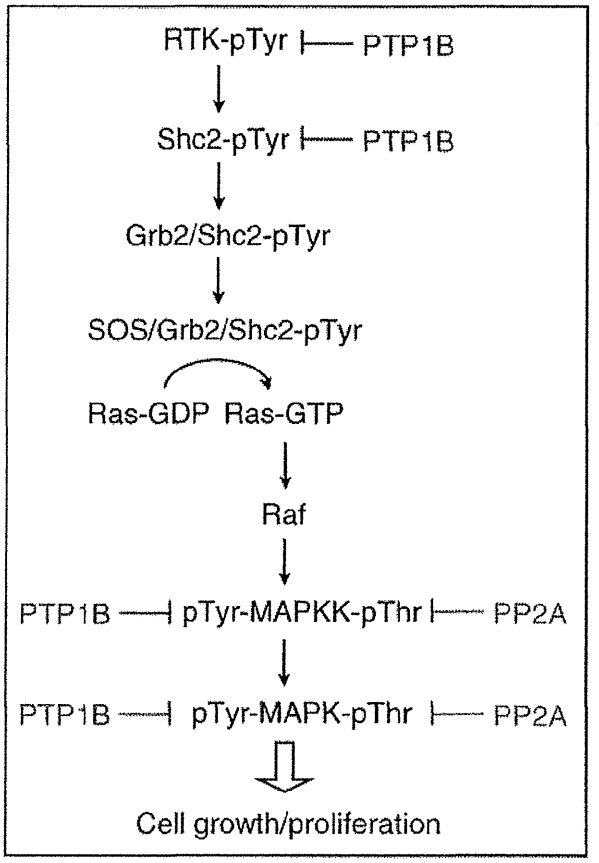

Figure 1. *A schematic pathway for receptor tyrosine kinase (RTK)-related mitogen-activated protein (MAP) kinase (MAPK) activation pathway. SHC2, Src-homology and collagen homology 2; GRB2, growth factor receptor binding protein 2; SOS, son of sevenless; MAPKK, MAPK kinase; PP2A, protein phosphatase 2A; PTP1B, protein tyrosine phosphatase 1B.*

Western blotting. Cells were treated or not with DPPE, and then lysed in a lysate solution [150 mM NaCl, 20 mM Tris, 0.1% (v/v) Tween-20 and 0.1% (w/v) sodium dodecyl sulfate (SDS), pH 7.5] containing 1% (v/v) protease inhibitor cocktail and 1% (v/v) phosphatase inhibitor cocktail. The lysates were centrifuged at 3,000 rotation per minute (rpm) for 5 min at 4°C. Proteins were separated by SDS polyacrylamide gel electrophoresis (PAGE) using a TGX gel (BioRad, Hercules, CA, USA) and then transferred to polyvinylidene difluoride (PVDF) membranes. Blotted membranes were blocked with TBS-T [150 mM NaCl, 0.1% (v/v) Tween-20 and 20 mM Tris, pH 7.5] containing 5% (w/v) bovine serum albumin and subsequently reacted with antibodies against phospho-MEK (pMEK) (Cell Signaling Technology, Inc., Danvers, MA, USA), MEK (Cell Signaling Technology), phospho-ERK1/2 (pERK1/2)(Santa Cruz Biotechnology, Santa Cruz, CA, USA), and ERK (Santa Cruz Biotechnology). After

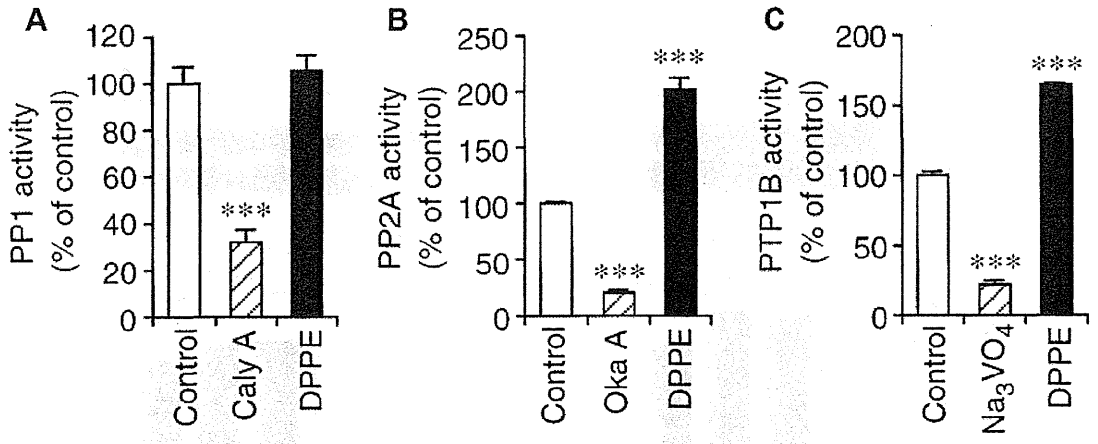

Figure 2. *Effects of 1,2-dipalmitoleoyl-sn-glycero-3-phosphoethanolamine (DPPE) on activities of protein phosphatase 1 (PP1) (A), protein phosphatase 2A (PP2A) (B), and protein tyrosine phosphatase 1B (PTP1B) (C). PP1, PP2A, or PTP1B was reacted separately with p-nitrophenyl phosphate (pNPP) in the presence and absence of 1,2-dipalmitoleoyl-sn-glycero-3-phosphoethanolamine (DPPE) (100 μM) with and without calyculin A (Caly A) (20 nM), okadaic acid (Oka A) (2 nM), or sodium orthovanadate (Na_3VO_4) (1 μM), and dephosphorylated pNPP was quantified. In the graphs, each value represents the mean (±SEM) percentage of basal phosphatase activity (control) (n=4 independent experiments). ***p<0.0001 as compared with control, Dunnett's test.*

washing, membranes were reacted with a horseradish peroxidase-conjugated goat anti-mouse IgG or goat anti-rabbit IgG antibody. Immunoreactivity was detected with an ECL kit (Invitrogen, Carlsbad, CA, USA) and visualized using a chemiluminescence LAS-4000 mini detection system (GE Healthcare). Protein concentrations for each sample were determined with a BCA protein assay kit (Thermo Fisher Scientific, Waltham, MA, USA).

Statistical analysis. Statistical analysis was carried out using Dunnett's test, and $p<0.01$ was regarded as significance.

Results

DPPE enhances PP2A and PTP1B activities. We initially examined the effects of DPPE (100 μM) on protein phosphatases. In the PP1 assay, calyculin A (20 nM), an inhibitor of PP1, clearly reduced PP1 activity (Figure 1A), confirming a reliable PP1 assay. No significant effect on PP1 activity was obtained with DPPE (Figure 2A).

In the PP2A assay, okadaic acid (2 nM), an inhibitor of PP2A, clearly reduced PP2A activity (Figure 2B), confirming a reliable PP2A assay. DPPE significantly enhanced PP2A activity, reaching nearly twice that of the control levels (Figure 2B).

In the PTP1B assay, sodium orthovanadate (Na_3VO_4) (1 μM), an inhibitor of PTP1B, clearly attenuated PTP1B activity (Figure 2C), confirming a reliable PTP1B assay. DPPE significantly enhanced PTP1B activity, reaching approximately 1.6 fold that of the control levels (Figure 2C).

DPPE tends to attenuate ERK1/2 activity in NCI-H28 cells. If DPPE enhances PP2A and PTP1B activities, then the lipid should suppress activities of MEK and ERK1/2. To address whether DPPE affects protein phosphatase activities, we monitored phosphorylation of MEK and ERK1/2 in Met5A non-malignant mesothelial cells and NCI-H28 malignant mesothelioma cells.

DPPE (100 μM) reduced phosphorylation of MEK in a treatment time (10-60 min)-dependent manner in Met5A cells, but phosphorylation of ERK1/2 was little affected (Figure 3A). DPPE (100 μM) had little effect on phosphorylation of MEK, but reduced phosphorylation of ERK1/2 in a treatment time (10-60 min)-dependent manner in NCI-H28 cells (Figure 3B). The potential for the inhibitory effect of DPPE on phosphorylation of MEK and ERK1/2, however, was much lower than expected and not significant.

DPPE induces apoptosis of NCI-H28 cells. In the MTT assay, treatment with DPPE for 24-48 h reduced NCI-H28 cell viability in a concentration (1-100 μM)-dependent manner, but had no effect on Met5A cell viability (Figure 4). This indicates that DPPE induces cell death in NCI-H28 malignant mesothelioma cells, but not Met5A non-malignant mesothelial cells.

To determine whether the effect of DPPE was due to apoptosis, we finally carried out TUNEL staining. DPPE (30 and 100 μM) significantly increased the number of TUNEL-positive cells as compared with those for untreated control NCI-H28 cells (Figure 5). DPPE at a concentration of 100 μM significantly increased the number of TUNEL-positive Met5A cells, but to a much lesser extent than that for NCI-H28 cells (Figure 5). Taken together, these results indicate that DPPE induces apoptosis of NCI-H28 malignant mesothelioma cells rather than Met5A non-malignant mesothelial cells.

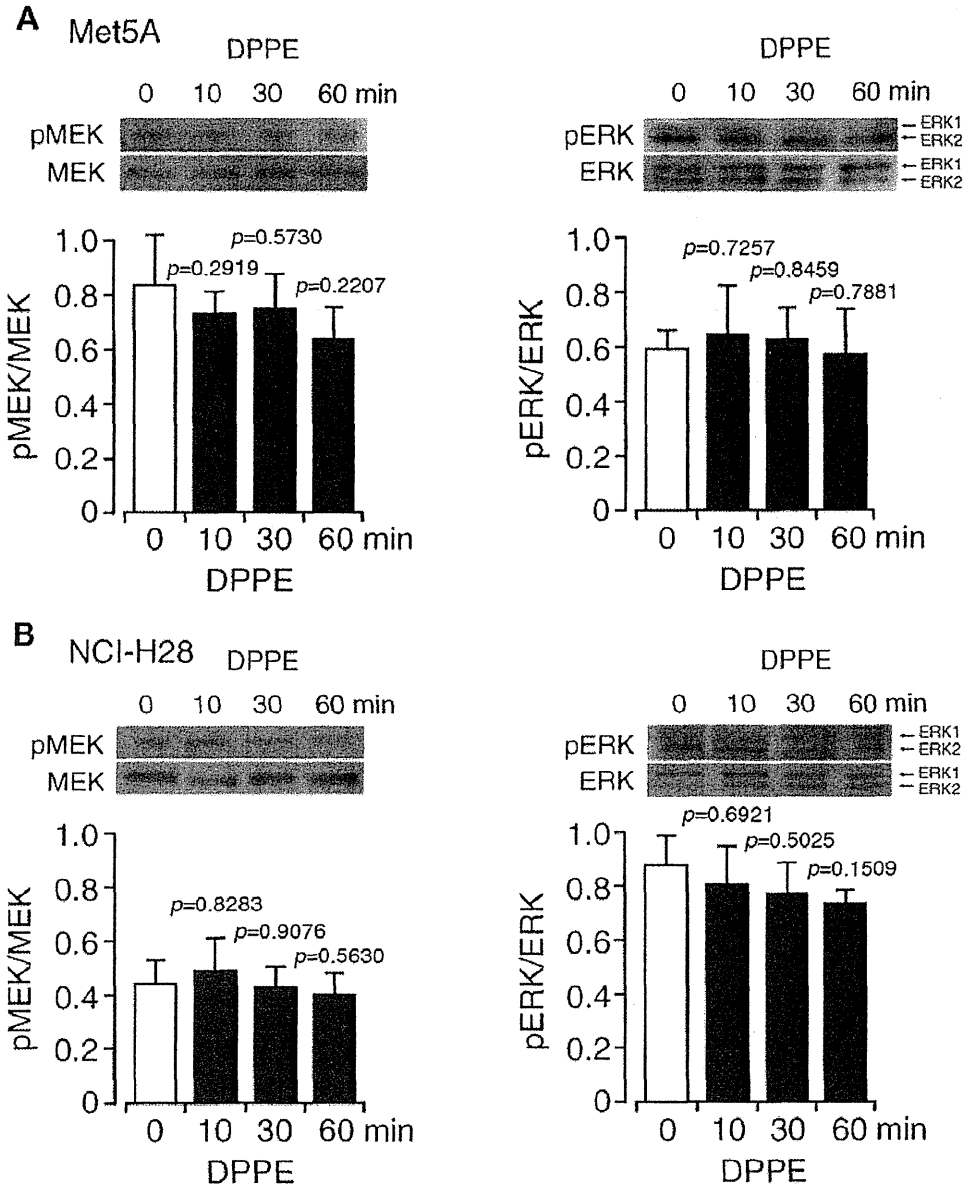

Figure 3. *Effects of 1,2-dipalmitoleoyl-sn-glycero-3-phosphoethanolamine (DPPE) on activity of mitogen-activated protein kinase kinase (MEK) and extracellular signal-regulated kinase (ERK). Met5A (A) and NCI-H28 (B) cells were treated with DPPE (100 μM) for the indicated periods of time, followed by western blotting using antibodies against pMEK, MEK, pERK1/2, and ERK1/2. In the graphs, each column represents the mean (±SEM) ratio of signal intensity of phosphorylated protein relative to MEK signal intensity or that of non-phosphorylated protein (n=4 independent experiments). p-Values were defined by Dunnett's test.*

Discussion

The phospholipid PE is the most abundant lipid in the cytoplasmic layer of cellular membranes and PE is implicated in a wide range of cellular processes such as membrane fusion, cell cycle, autophagy, apoptosis, and cognitive function (5-9).

PE is produced through three main pathways: the cytidine 5'-diphosphate (CDP)-ethanolamine Kennedy pathway, mitochondrial phosphatidylserine (PS) decarboxylation pathway catalyzed by PS decarboxylase, and acylation of lysoPE catalyzed by lysophosphatidylethanolamine acyltransferase. The CDP-ethanolamine Kennedy pathway is the only route for *de novo* synthesis of PE (10).

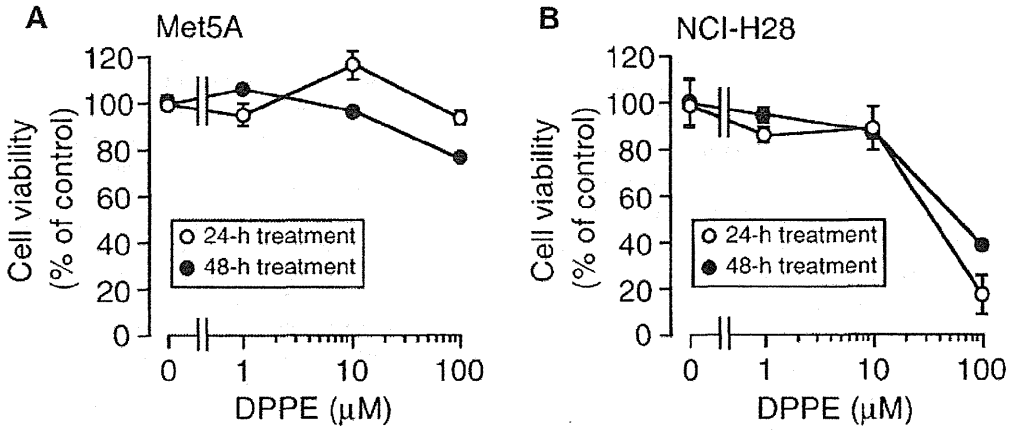

Figure 4. *Effects of 1,2-dipalmitoleoyl-sn-glycero-3-phosphoethanolamine (DPPE) on cell viability. 3-(4,5-Dimethyl-2-thiazolyl)-2,5-diphenyl-2H-tetrazolium bromide (MTT) assay was carried out on Met5A (A) and NCI-H28 (B) cells treated with DPPE at the concentrations indicated for 24-48 h. In the graphs, each point represents the mean (±SEM) percentage of control cell viability (MTT intensity of cells not treated with DPPE) (n=4 independent experiments).*

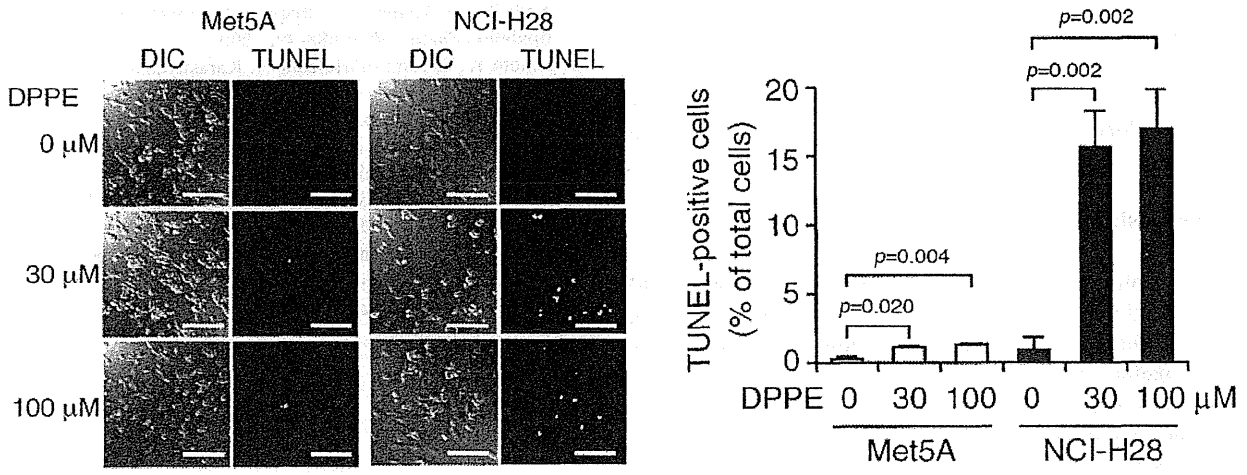

Figure 5. *Terminal deoxynucleotidyl transferase-mediated dUTP nick-end labeling (TUNEL) staining. TUNEL staining was carried out on Met5A and NCI-H28 cells treated with 1,2-dipalmitoleoyl-sn-glycero-3-phosphoethanolamine (DPPE) at the concentrations indicated for 48 h. DIC, Differential interference contrast. Bars=100 μm. TUNEL-positive cells were counted in an area (0.4 mm × 0.4 mm) selected at random. In the graph, each column represents the mean (±SEM) percentage of TUNEL-positive cells relative to the total number of cells (n=4 independent experiments). p-Values were defined from Dunnett's test.*

Phosphorylation of ethanolamine by ethanolamine kinase is followed by the CTP:choline cytidylyltransferase 2 (PCyt2)-mediated production of CDP-ethanolamine, and PE production is catalyzed by CDP-ethanolamine:1,2-diacylglycerol ethanolaminephosphotransferase. The analogous enzymes of the CDP-choline branch of the Kennedy pathway include choline kinase, PCyt1, and CDP-choline:1,2-diacylglycerol choline phosphotransferase. In the liver, PE is transformed into phosphatidylcholine (PC) catalyzed by PE N-methyltransferase. PE is also produced in mitochondria by PS decarboxylase-catalyzed decarboxylation of PS. Mammals do not synthesize PS *de novo*, and therefore, PS is produced by head-group exchange from PE catalyzed by PS synthase-2 or PC catalyzed by PS synthase-1. PE, on the other hand, is produced by lysoPE acyltransferase-catalyzed fatty acid esterification of lysoPE.

In the present study, DPPE, a PE, enhanced PP2A and PTP1B activities. To our knowledge, this is the first to show the new action of PE on protein phosphatases. How DPPE enhances PP2A and PTP1B activities, however, remains to be determined. Activation of ERK, a MAPK, leads to promotion of cell growth and proliferation not only of normal cells but also of cancer cells. Activation of ERK1/2 through a pathway along the RTK/(SHC2/GRB2/SOS)/RAS/RAF/MAPKK/MAPK axis is initiated by tyrosine phosphorylation of RTK and SHC2 (Figure 1). PTP1B dephosphorylates RTK, SHC2, MAPKK, and MAPK, thereby negatively-regulating RTK signaling (Figure 1). PP2A dephosphorylates and inactivates, MAPKK, and MAPK (Figure 1). Accordingly, DPPE, in order to enhance PP2A and PTP1B activities, should attenuate RTK signaling and inhibit ERK activation. Indeed, DPPE tended to reduce pMEK in Met5A cells and pERK1/2 in NCI-H28 cells at 60-min treatment, but the potential was much lower than expected.

Strikingly, DPPE clearly reduced cell viability and markedly increased TUNEL-positive NCI-H28 malignant mesothelioma cells. In contrast, DPPE had little effect on cell viability and the number of TUNEL-positive cells for Met5A non-malignant mesothelial cells. DPPE, thus, appears to preferentially induce apoptosis of NCI-H28 cells, but not of Met5A cells. This raises the possibility that DPPE could be developed as an anticancer drug for treatment of malignant mesothelioma.

Conclusion

The results of the present study demonstrate that DPPE preferentially induces apoptosis of NCI-H28 malignant mesothelioma cells rather than Met5A non-malignant mesothelial cells. DPPE enhanced PP2A and PTP1B activities in a cell-free system, and this action might, at least in part, contribute to DPPE-induced apoptosis of malignant mesothelioma cells.

Conflicts of Interest

None of the Authors have any potential conflict of interest.

References

1 Raja S, Murthy SC and Mason DP: Malignant pleural mesothelioma. Curr Oncol Rep *13*: 259-264, 2011.

2 Kanno T, Tsuchiya A, Shimizu T, Tanaka A and Nishizaki T: Indomethacin serves as a potential inhibitor of protein phosphatases. Cell Physiol Biochem *30*: 1014-1022, 2012.

3 Yaguchi T, Muramoto M, Nakano T and Nishizaki T: Urinary trypsin inhibitor suppresses migration of malignant mesothelioma. Cancer Lett *288*: 214-218, 2010.

4 Nogi Y, Kanno T, Nakano T, Fujita Y, Tabata C, Fukuoka K, Gotoh A and Nishizaki T: AMP converted from intracellularly transported adenosine up-regulates p53 expression to induce malignant pleural mesothelioma cell apoptosis. Cell Physiol Biochem *30*: 61-74, 2012.

5 Deeba F, Tahseen HN, Sharad KS, Ahmad N, Akhtar S, Saleemuddin M and Mohammad O: Phospholipid diversity: Correlation with membrane-membrane fusion events. Biochim Biophys Acta *1669*: 170-181, 2005.

6 Emoto K, Kobayashi T, Yamaji A, Aizawa H, Yahara I, Inoue K and Umeda M: Redistribution of phosphatidylethanolamine at the cleavage furrow of dividing cells during cytokinesis. Proc Natl Acad Sci USA *93*: 12867-12872, 1996.

7 Ichimura Y, Kirisako T, Takao T, Satomi Y, Shimonishi Y, Ishihara N, Mizushima N, Tanida I, Kominami E, Ohsumi M, Noda T and Ohsumi Y: A ubiquitin-like system mediates protein lipidation. Nature *408*: 488-492, 2000.

8 Emoto K, Toyama-Sorimachi N, Karasuyama H, Inoue K and Umeda M: Exposure of phosphatidylethanolamine on the surface of apoptotic cells. Exp Cell Res *232*: 430-434, 1997.

9 Yaguchi T, Nagata T and Nishizaki T: 1,2-dilinoleoyl-sn-glycero-3-phosphoethanolamine ameliorates age-related spatial memory deterioration by preventing neuronal cell death. Behav Brain Funct *6*: 52.doi:10.1186/1744-9081-6-52, 2010.

10 Pavlovic Z and Bakovic M: Regulation of phosphatidylethanolamine homeostasis – The critical role of CTP: phosphoethanolamine cytidylyltransferase (Pcyt2). Int J Mol Sci *14*: 2529-2550, 2013.

Received October 15, 2013
Revised November 7, 2013
Accepted November 11, 2013

Int J Clin Oncol (2014) 19:45–49
DOI 10.1007/s10147-012-0515-4

ORIGINAL ARTICLE

Frequency of epidermal growth factor receptor mutations in Bangladeshi patients with adenocarcinoma of the lung

Shakibur Rahman · Nobuyuki Kondo · Kazue Yoneda · Teruhisa Takuwa · Masaki Hashimoto · Hayato Orui · Yoshitomo Okumura · Fumihiro Tanaka · Kanako Kumamoto · Mohammad Golam Mostafa · Golam Mohiuddin Akbar Chowdhury · Akramul Haque · Seiki Hasegawa

Received: 27 July 2012 / Accepted: 18 December 2012 / Published online: 9 January 2013

Abstract
Background Worldwide studies on lung adenocarcinoma have demonstrated a genetic divergence of the epidermal growth factor receptor (EGFR) pathway according to ethnicity, such as higher frequency of activated EGFR mutations among East Asian patients. However, such information is still lacking in some developing countries.
Methods We investigated the frequency of EGFR mutations among Bangladeshi patients with adenocarcinoma of the lung. Fine-needle aspiration tissue samples were collected from 61 Bangladeshi patients. Polymerase chain reaction–single-strand conformation polymorphism was performed on extracted DNA for mutational analysis of EGFR exons 19 and 21.
Results EGFR mutations were found in 14 of 61 (23.0 %) Bangladeshi patients. There was no significant difference in EGFR mutation rate with regard to patient's age, sex, smoking history, clinical stage of lung cancer, subtypes of adenocarcinoma, and tumor differentiation.
Conclusion The present study revealed that the EGFR mutation rate in Bangladeshi patients with adenocarcinoma of the lung was higher than in African–American, Arabian, and white Caucasian patients, and was lower than in East Asia.

Keywords Lung cancer · Epidermal growth factor receptor · EGFR mutation · Tyrosine kinase inhibitors · Single-strand conformation polymorphism · Ethnic difference

S. Rahman · N. Kondo · K. Yoneda · T. Takuwa · M. Hashimoto · H. Orui · S. Hasegawa (✉)
Department of Thoracic Surgery, Hyogo College of Medicine, 1-1 Mukogawa-cho, Nishinomiya, Hyogo 663-8501, Japan
e-mail: hasegawa@hyo-med.ac.jp

Y. Okumura
Department of Thoracic Surgery, Itami City Hospital, Koyaike 1-100, Itami 664-8540, Japan

F. Tanaka
Second Department of Surgery, University of Occupational and Environmental Health, Iseigaoka 1-1, Kitakyusyu 807-8555, Japan

K. Kumamoto
Department of Genetic Disease Research, Graduate School of Medicine, Osaka City University, Asahimachi 1-5-7, Osaka 545-8586, Japan

M. G. Mostafa
Department of Pathology, National Institute of Cancer Research and Hospital (NICRH), Mohakhali, Dhaka 1212, Bangladesh

G. M. A. Chowdhury · A. Haque
Department of Thoracic Surgery, National Institute of Diseases of the Chest and Hospital (NIDCH), Mohakhali, Dhaka, Bangladesh

Introduction

The frequency of epidermal growth factor receptor (EGFR) mutation in non-small cell lung cancer is documented to differ across ethnic groups, with a notably higher occurrence observed in East-Asian trials (30–60 %) and a lower occurrence in North-American studies (10–20 %) [1–4]. The reasons for ethnic influence on mutation incidence still remain poorly understood.

Several reports suggest that EGFR mutations provide survival benefit independent of treatment [5, 6]. More recent information focussing on East Asia also suggests that the presence of classical EGFR mutations is predictive of survival benefit after EGFR tyrosine kinase inhibitor (TKI) therapy [7].

Since there are no reports of genetic backgrounds of lung cancer in Bangladesh, we examined the frequency of major types of activating mutations (exons 19 and 21) of EGFR in Bangladeshi patients with adenocarcinoma of the lung.

Patients and methods

Clinical characteristics of patients

A total of 61 patients underwent computed tomography (CT)-guided fine-needle aspiration (FNA) biopsy at the National Institute of Diseases of the Chest and Hospital (NIDCH), National Institute of Cancer Research and Hospital (NICRH), and related diagnostic centers in Bangladesh from 2009 to 2011. Written informed consent was obtained from each patient.

The clinical information on these patients is shown in Table 1. None of the patients were exposed to any chemotherapy before FNA. Pathological diagnoses were performed by pathologists, unaware of the clinical information, and finally confirmed by one pathologist (M.G.M.) according to the WHO classification system [8].

Table 1 Characteristics of the 61 patients included in the study

Variable	All patients
Age (years)	Median 56.5 (range 18–95)
Gender	
Male	47 (77 %)
Female	14 (23 %)
Smoking status	
Never-smoker	23 (38 %)
Former-smoker	8 (13 %)
Current-smoker	30 (49 %)
Brinkman index	
Former-smoker	593
Current-smoker	878
Clinical stage	
Stage I	7 (11 %)
Stage II	17 (28 %)
Stage III	17 (28 %)
Stage IV	20 (33 %)

FNA sample and DNA

CT-guided FNA biopsies were performed using 23-gauge needles in all patients. Suitability for DNA extraction was recognized when pathologists confirmed that more than 70 % of each sample consisted of tumor cells.

FNA samples were immediately preserved in tubes containing 99.5 % ethanol at −80 °C. Genomic DNA was isolated from tissue by discarding the ethanol after centrifugation at high speed. Genomic DNA was extracted using the EZ1 DNA Tissue Kit with the EZ1 instrument (QIAGEN, Germany).

Polymerase chain reaction–single-strand conformation polymorphism (PCR–SSCP) was used to detect mutations in exons 19 and 21 of the EGFR gene. PCR was performed using the AmpliTaq Gold PCR Master Mix (Life Technologies, USA). The primers used and PCR conditions are shown in Table 2. After denaturing PCR products, electrophoresis was performed with the GenePhor System and GeneGel Excel 12.5/24 (GE Healthcare, Sweden) at 18 °C, 650 V for 80 min. The gels were stained using the DNA Silver Staining Kit (GE).

Statistical analysis

The incidence of EGFR mutation status along with the corresponding important predictors of incidence of EGFR mutations were additionally identified by logistic regression with a forward-model selection procedure. The factors included in the model selection were age, sex, histology, and tumor stage. The differences in continuous measurements between two groups were examined by the t test or Fisher's exact test, and the Mann–Whitney U test was used to determine the differences between continuous variables. All tests were two-sided, and $P < 0.05$ was considered statistically significant.

Results

Out of 61 tumors, mutations in exons 19 and 21 of the EGFR gene were detected in 8 (13.1 %) and 6 (9.8 %)

Table 2 PCR primers and parameters

EGFR gene	Forward (5′–3′)	Reverse (5′–3′)	Product size (bp)	Number of cycle	Annealing condition
Exon19	CGTCTTCCTTCTCTCTCTGT	CCACACAGCAAAGCAGAAAC	148	35	55 °C, 15 s
Exon21	AGGGCATGAACTACTTG	CCTCCTTACTTTGCCTCCTTC	167	35	55 °C, 15 s